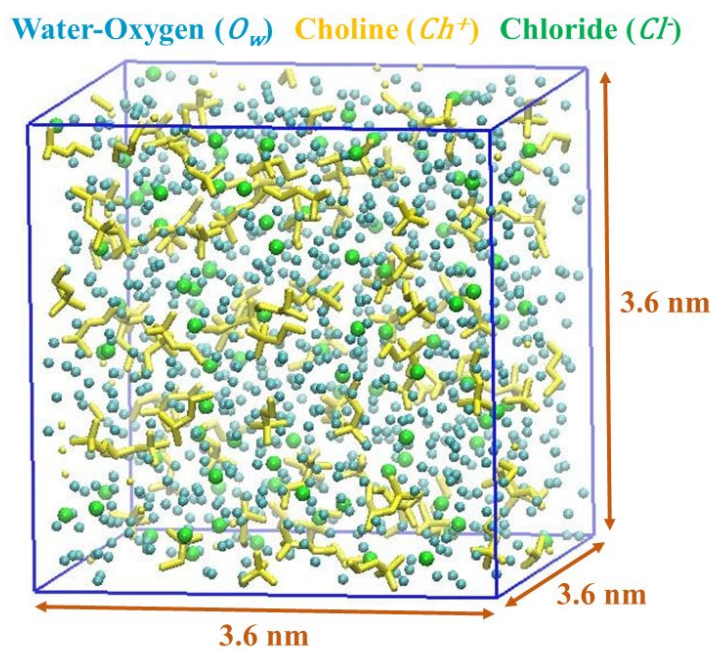Supporting Information for

In silico Elucidation of Molecular Picture of Water-Choline Chloride Mixture

Soham Sarkar, Atanu Maity, and Rajarshi Chakrabarti*

Department of Chemistry, Indian Institute of Technology Bombay, Powai, Mumbai-400076, India

E-mail: rajarshi@chem.iitb.ac.in

Fig S1: Representative snapshot of the simulation box filled with Water-Oxygen (Cyan), Choline (Yellow) and Chloride (Green). All constituents are represented in licorice. For the sake of visual clarity, hydrogen atoms are not shown.

System Identifier	No. of water molecules	No. of choline ions	No. of chloride ions	Simulation length (ns)	Density (kg/m³)	
					Experimental (308.15 K)	Simulated (310 K)
W	1636	--	--	50	--	--
W-C (1M)	1404	30	30	50	1011.91	1010.11
W-C (2M)	1163	60	60	50	1030.16	1028.15
W-C (3M)	929	90	90	50	1057.99	1046.75
W-C (4M)	703	120	120	50	1179.19	1060.72

Table S1: Details of the composition of solvent/co-solvent in different systems and their simulation length. Experimental densities of the investigated aqueous solutions of choline chloride is taken from Shaukat *et al.*[1]

| Atom name	Abbreviation used in the plot
Oxygen atom of water	O_w
Hydrogen atom of water	H_w
Hydroxyl Oxygen of Choline cation	$O_{Ch}{}^+$
Hydroxyl Hydrogen of Choline cation	$OH_{Ch}{}^+$
Nitrogen of Choline cation	$N_{Ch}{}^+$
Chloride ion	Cl^-

**Table S2:** Abbreviations used in this manuscript for different atoms in the plots.
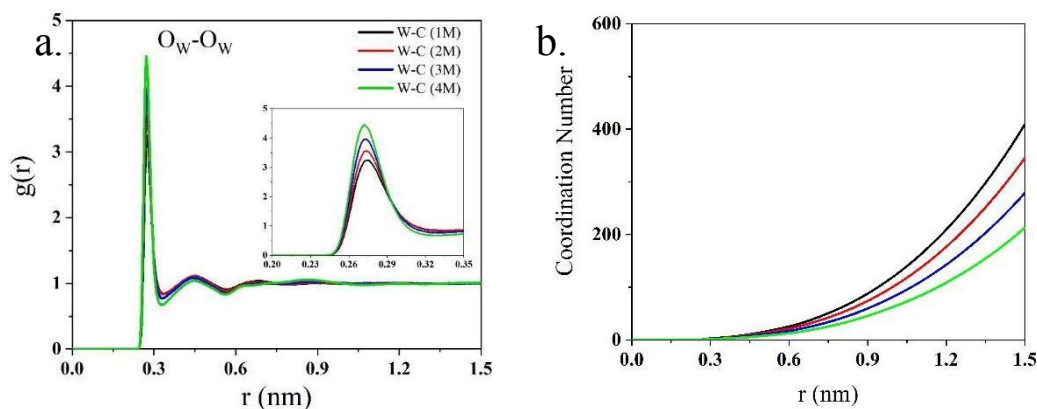
Fig S2: a) Radial distribution functions ($g(r)$) and **b)** coordination calculated for water-oxygen (O_w) around water-oxygen (O_w) for different systems under study. The relevant part of Fig S2a is magnified and shown in the inset.

A close observation of Fig S2a depicts the existence of a sharp and single peak ~0.275nm (magnified in the inset) which is observed in all systems for the distribution of O_w around O_w. The position of this particular peak is also experimentally and computationally verified by earlier studies.[2–4]

With an increase in the amount of choline chloride in the system (*W-C (1M)* to *W-C (4M)*), water-oxygen atoms (O_w) approach each other as evident from Fig S2a and the *g(r)* value increases. Fig S2a clearly shows that though the position of the *g(r)* peak is the same for each system, the introduction of extra choline chloride pushes water molecules towards themselves. The probable reason lies behind this increase is the crowding induced by bulky choline and chloride ions on the water molecules. In our earlier publication[5], we have witnessed a similar trend for this particular atom-pair self-distribution but owing to the existence of the urea molecules in the system additional crowding present there. That causes extra compactness thereby water molecules come closer to each other to a higher extent compared to the binary mixture considered in the present investigation. For better understanding we have also provided the coordination number (Fig S2b) next to Fig S2a.
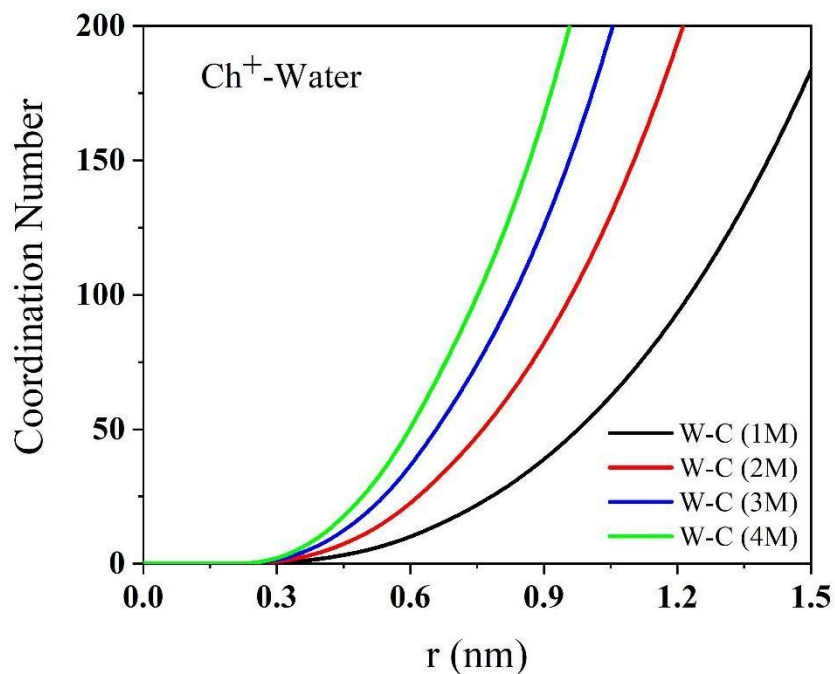

Fig S3: Coordination numbers calculated from the center-of-mass radial distribution functions (*g(r)*) of choline cation around water for different systems, showing higher accumulation of *Ch*$^+$ around water with increasing concentration.
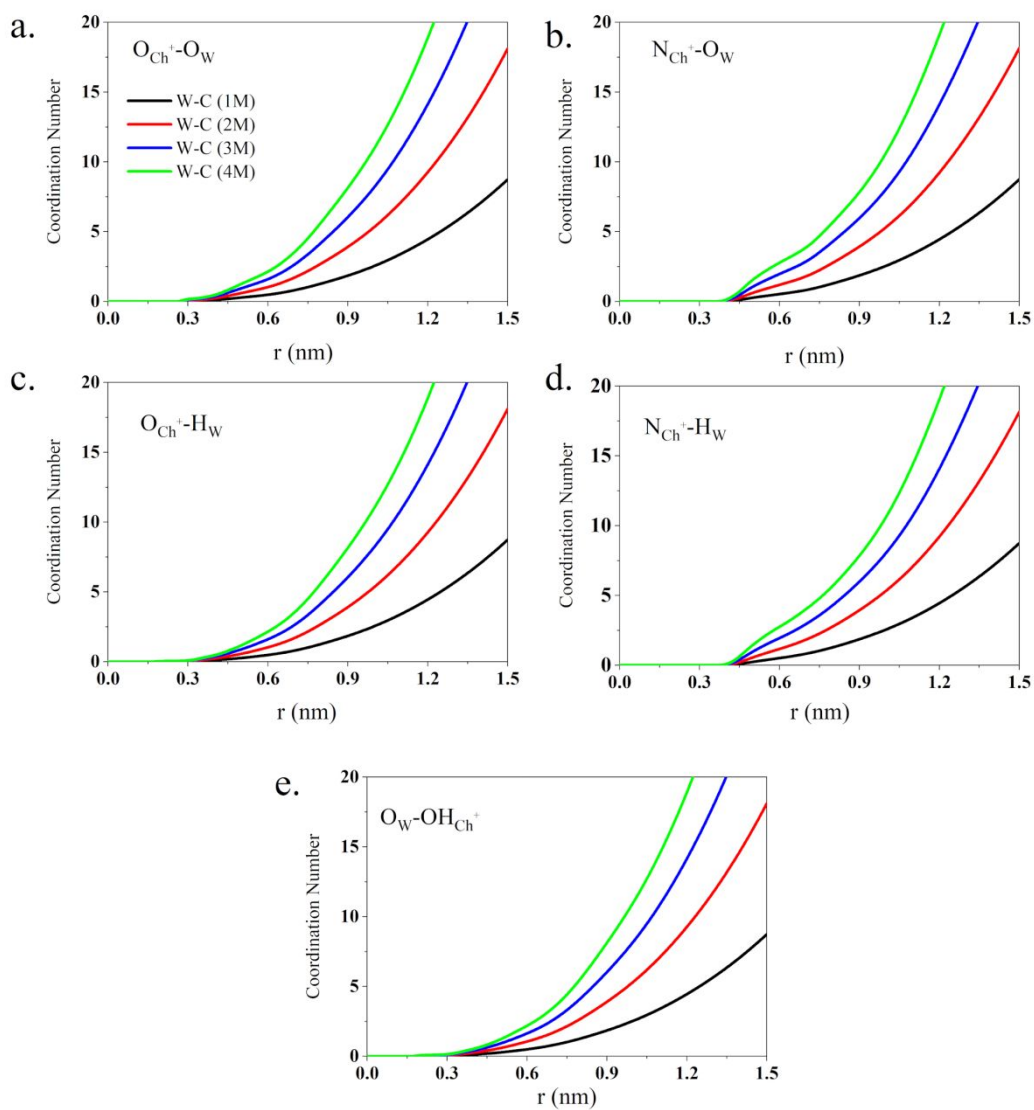
Fig S4: Coordination numbers calculated from the ($g(r)$) of **a)** O_{Ch^+}-O_W, **b)** N_{Ch^+}-O_W, **c)** O_{Ch^+}-H_W, **d)** N_{Ch^+}-H_W and **e)** O_W-OH_{Ch^+} for different systems.
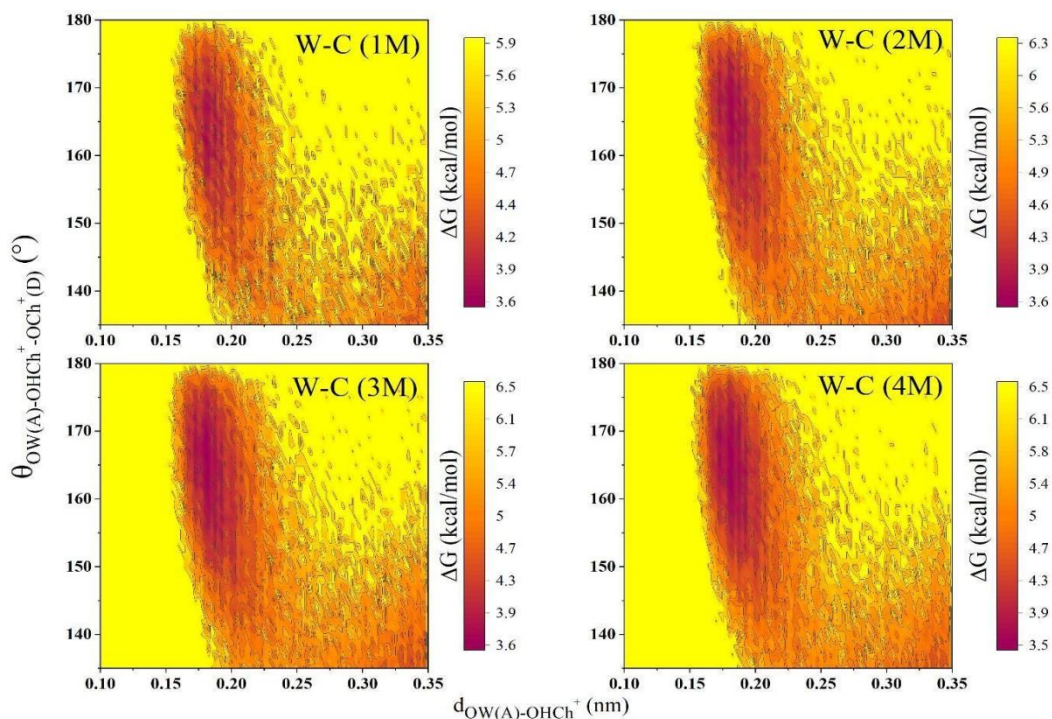
Fig S5a: Radial-Angular Distribution Functions (RADFs) calculated between the pair of Donor (O_{Ch}^+) – Acceptor (O_W). The hydrogen atom involved is the Hydroxyl Hydrogen (OH_{Ch}^+) of Choline cation. (A) = Acceptor, (D) = Donor.
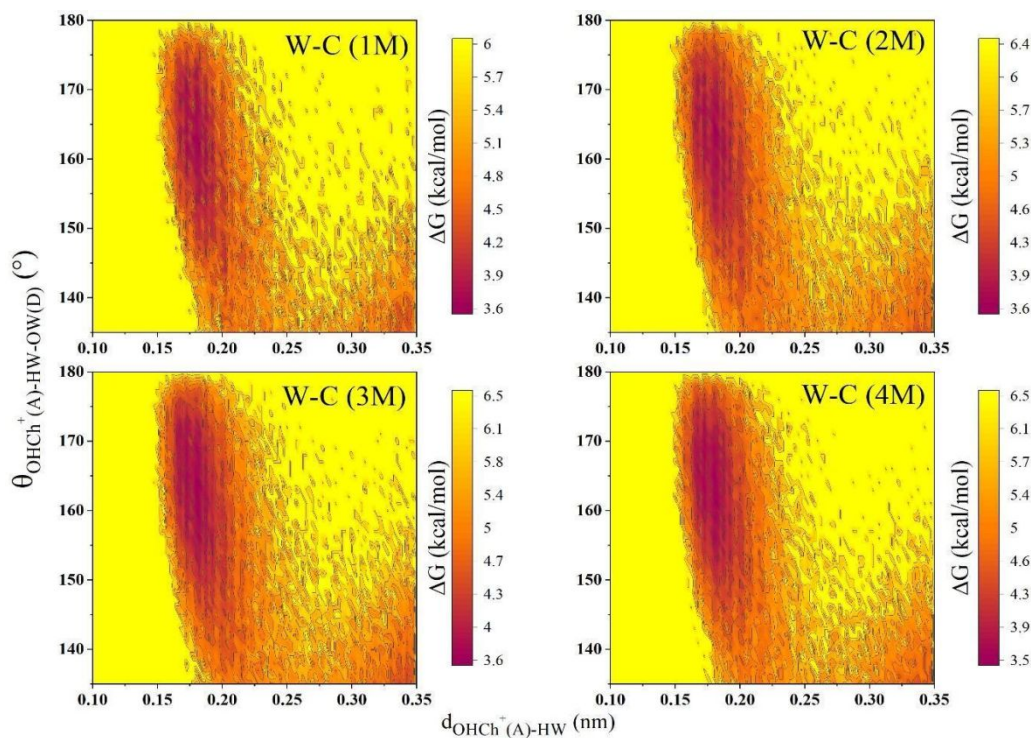
Fig S5b: Radial-Angular Distribution Functions (RADFs) calculated between the pair of Donor (O_W) – Acceptor (O_{Ch}^+). The hydrogen atom involved is the Hydrogen (H_W) of water. (A) = Acceptor, (D) = Donor.
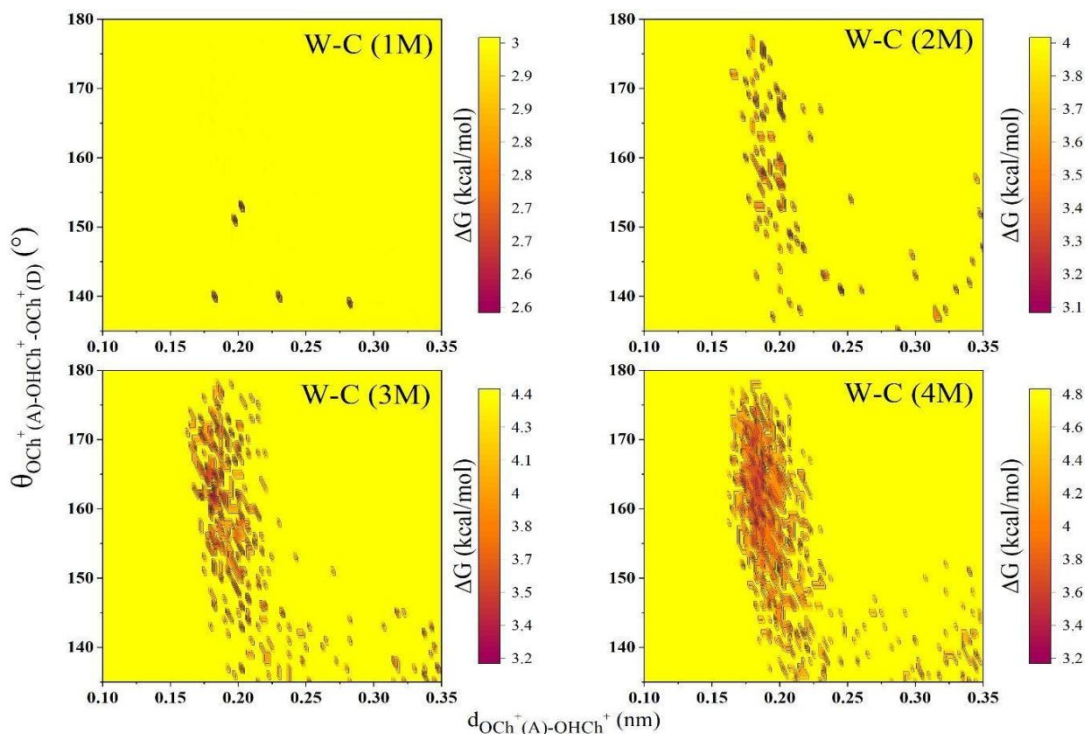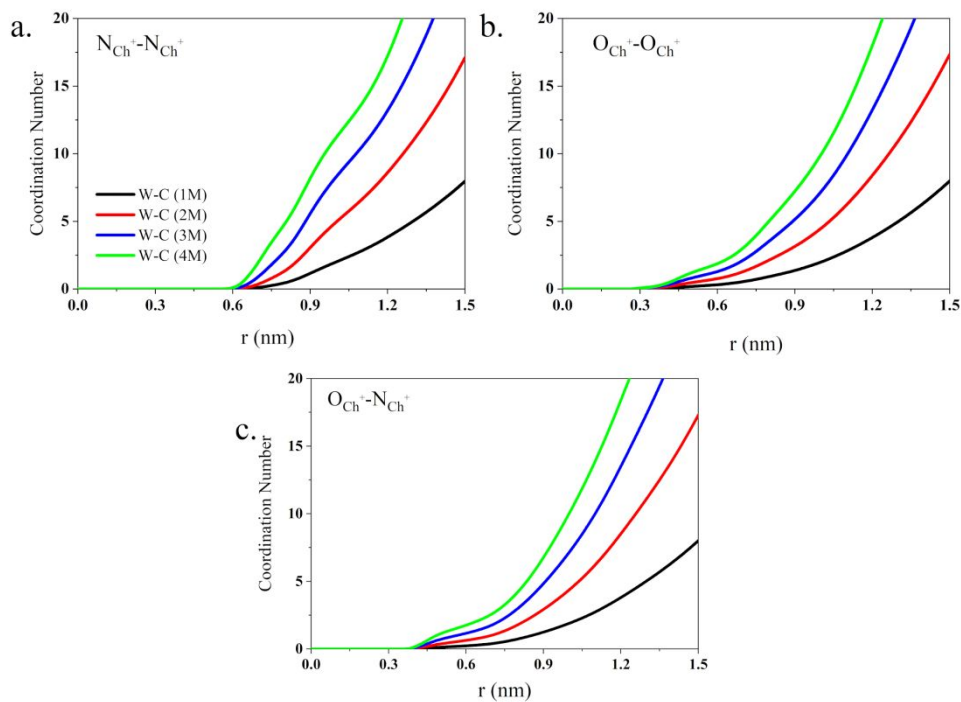
Fig S5c: Radial-Angular Distribution Functions (RADFs) calculated between the pair of Donor (O_{Ch}^+) – Acceptor (O_{Ch}^+). The hydrogen atom involved is the Hydroxyl Hydrogen (OH_{Ch}^+) of Choline cation. (A) = Acceptor, (D) = Donor.

Fig S6: Coordination numbers calculated from the radial distribution functions ($g(r)$) of **a)** N_{Ch}^+-N_{Ch}^+, **b)** O_{Ch}^+-O_{Ch}^+ and **c)** O_{Ch}^+-N_{Ch}^+ atom-pairs for different systems under study.

Bonding statistics			Identifier
Mono coordinated water molecules			
Water	Choline	Chloride	
1	0	0	1W-0Ch-0Cl
0	1	0	0W-1Ch -0Cl
0	0	1	0W-0Ch -1Cl
Bi coordinated water molecules			
Water	Choline	Chloride	
2	0	0	2W-0Ch -0Cl
0	2	0	0W-2Ch -0Cl
0	0	2	0W-0Ch -2Cl
1	1	0	1W-1Ch -0Cl
1	0	1	1W-0Ch -1Cl
0	1	1	0W-1Ch -1Cl
Tri coordinated water molecules			
Water	Choline	Chloride	
3	0	0	3W-0Ch -0Cl
0	3	0	0W-3Ch -0Cl
0	0	3	0W-0Ch -3Cl
2	1	0	2W-1Ch -0Cl
1	2	0	1W-2Ch -0Cl
2	0	1	2W-0Ch -1Cl
1	0	2	1W-0Ch -2Cl
0	2	1	0W-2Ch -1Cl
0	1	2	0W-1Ch -2Cl
1	1	1	1W-1Ch -1Cl
Tetra coordinated water molecules			
Water	Choline	Chloride	
4	0	0	4W-0Ch -0Cl
0	4	0	0W-4Ch -0Cl
0	0	4	0W-0Ch -4Cl
3	1	0	3W-1Ch -0Cl
1	3	0	1W-3Ch -0Cl
3	0	1	3W-0Ch -1Cl
1	0	3	1W-0Ch -3Cl
0	3	1	0W-3Ch -1Cl
0	1	3	0W-1Ch -3Cl
2	2	0	2W-2Ch -0Cl
2	0	2	2W-0Ch -2Cl
0	2	2	0W-2Ch -2Cl
2	1	1	2W-1Ch -1Cl
1	2	1	1W-2Ch -1Cl
1	1	2	1W-1Ch -2Cl

Table S3: Possible combinations of coordination of central water by water, urea, and choline for mono, bi, tri, and tetra coordinated water molecules. The coordination number indicates the number of successful hydrogen bonds with the central water molecule.
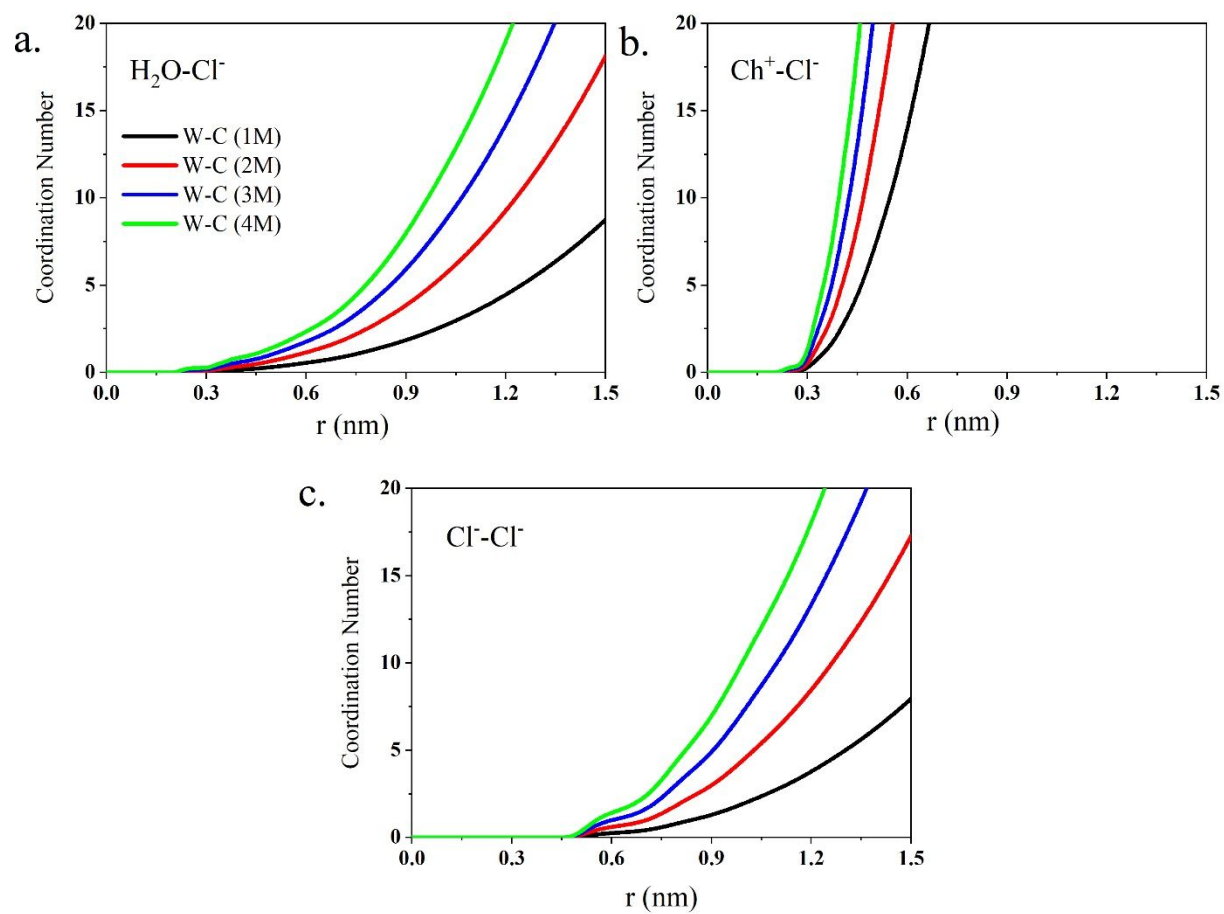
Fig S7: Coordination numbers of chloride (*Cl⁻*) around **a)** water (*H₂O*), **b)** choline (*Ch⁺*) and **c)** chloride (*Cl⁻*) around for different systems under study.
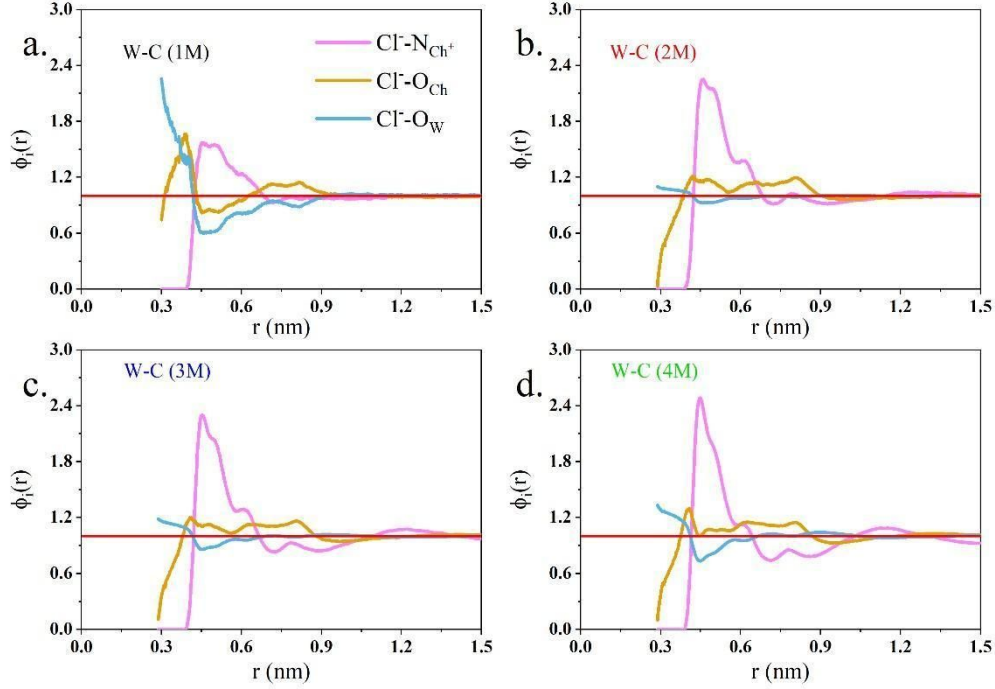
Fig S8: Relative number fraction $\Phi_i(r)$ of $N_{Ch}^+/O_{Ch}^+/O_w$ in (a) *W-C (1M)*, (b) *W-C (2M)*, (c) *W-C (3M)*, (d) *W-C (4M)* as a function of distance (r) from Cl^-, respectively.

Insights come from the quantification of the relative occupancy of space by the interacting components around Cl^-. O_{Ch}^+/O_w undergo hydrogen bonded interaction with Cl^-, whereas N_{Ch}^+ undergo electrostatic interaction with the chloride ion. We have calculated the relative number fraction ($\Phi_i(r)$) of $N_{Ch}^+/O_{Ch}^+/O_w$ surrounding Cl^- as we did in our earlier work.[5,6] $\Phi_i(r)$ is formulated as-

$$\Phi_i(r) = \frac{\dfrac{N_i(r)}{\sum_i N_i(r)}}{\dfrac{N_i(r_{Bulk})}{\sum_i N_i(r_{Bulk})}} \qquad (S1)$$

Here, $N_i(r)$ signifies the coordination number of $N_{Ch}^+/O_{Ch}^+/O_w$ around Cl^- and $N_i(r_{Bulk})$ is designated as the coordination number of $N_{Ch}^+/O_{Ch}^+/O_w$ around Cl^- at the bulk and $r_{Bulk} \gg 3$Å. The subscript i denotes the different components considered in the calculation, here N_{Ch}^+, O_{Ch}^+, and O_w. $\Phi_i(r) > 1$ signifies accumulation of that specific constituent with respect to bulk and $\Phi_i(r) < 1$ indicates exclusion.

It is evident from Fig S8 that at a short distance O_{Ch}^+ and O_w are complementing each other in terms of position. A close look into Fig S8 sheds light on the fact the bulkiness of the choline cation is somewhat hindering the Cl^- ion in the spontaneous access of the O_{Ch}^+ whereas in the case of O_w the interaction is possible as water molecule has no such hindrances. We find an initial accumulation of the O_w atoms around

the Cl^- anion whereas there is a net exclusion of the $O_{Ch}{}^+$ atoms at a short distance. The picture is completely reverse as we slightly move beyond. This ultimately produces a scenario of competitive hydrogen bond formation among these two donor sources with that of the Cl^- ion.

Further observation indicates that there is an accumulation ($\Phi_i(r) > 1$) of the $N_{Ch}{}^+$ around the Cl^- anion as we move a little bit higher. As the nitrogen atom ($N_{Ch}{}^+$) is heavily guarded by three methyl ($-CH_3$) groups, the peak position is found to reside around 0.45 nm, where the electrostatic interaction actively prevails as it is a long-range interaction. We find that the existence of the electrostatic interaction and thus $N_{Ch}{}^+$ successfully replace the oxygen atoms from the vicinity of the Cl^- ion. With an increase in the distance, we find a decrease in the $\Phi_i(r)$ value for all concentration (Fig S8, a-d), indicating a relative depletion of the interacting atoms, though their accumulating tendency exists as the $\Phi_i(r)$ shows value greater than 1 at a long distance also.

## Tetrahedral order Parameter (TOP)

Formulation and protocols

A widely used parameter to explore the microscopic structural details of water is the orientational tetrahedral order parameter[7–9] (q_{tet}). The working formula of q_{tet} is provided in the main manuscript.

For neat liquid water, four closest water-oxygen atoms (O_w) are considered around a central water-oxygen (O_w) and the angle subtended by two partners (i, k) with the central Ow (j) is designated as θ_{ijk}. $q_{tet} = 1$ indicates a perfectly tetrahedral ice-like structure whereas $q_{tet} = 0$ signifies a completely distorted orientation. We find a detailed explanation of equation S2 elsewhere.[10,11] For calculation purposes, we have considered the last 10 ns of the simulated trajectory.

Protocol	Atoms accounted as partner
Protocol-1	O_w
Protocol-2	O_w, $O_{Ch}{}^+$, $N_{Ch}{}^+$
Protocol-3	O_w, $O_{Ch}{}^+$, $N_{Ch}{}^+$, Cl^-

Table S4: List of atoms accounted for different protocols for calculation of q_{tet}
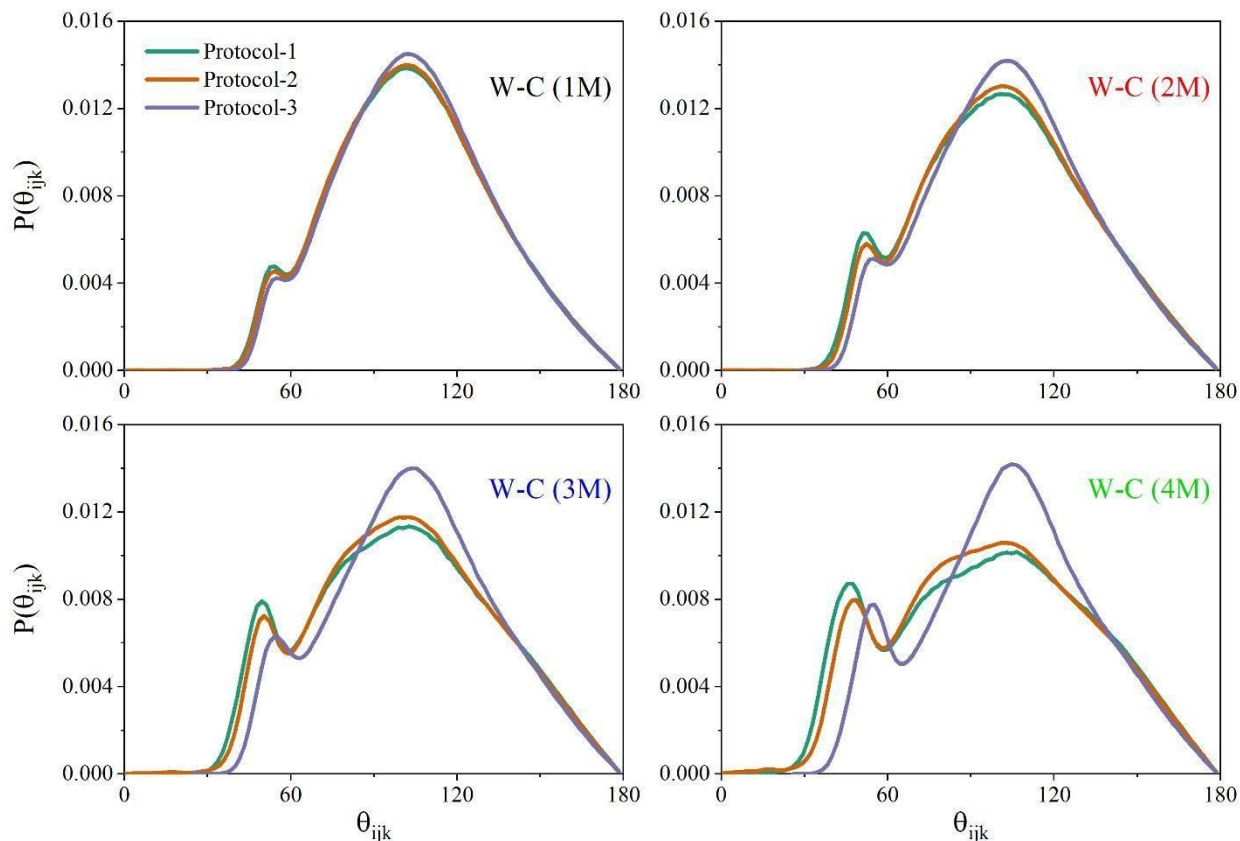
Fig S9: Probability distribution (P(θ_{ijk})) of angle θ_{ijk} subtended by two partners (i, k) with the central O_w (j) following (a) Protocol-1, Protocol-2 and Protocol-3 for all systems under investigation.

Fig S9 depicts the probability distribution of the subtended angle (θ_{ijk}) formed at the central water oxygen. We have represented the probability distribution plot using all three protocols used to calculate q_{tet}. The characteristic of this probability distribution is the coexistence of two peaks. The first one resides between 30° and 60° signifies a distorted structure of water and the second large one resides between 100° and 110° indicates tetrahedrality in water structure. Considering *W-C (1M)*, we see that plots obtained following three protocols are almost overlapping with each other. The reason for this observation is the sufficiently low concentration of choline chloride in the system hence negligible contribution comes from both the cation and anion as the partner of the central water molecule which effectively distinguishes the protocols used. The aforesaid justification is further supported by the fraction of contribution of the constituents (Fig 10, main manuscript). Increasing the concentration of the choline chloride leads to a flattening of the peak residing between 100° and 110° and an increase in first peak height following Protocol-1. This trend is similar for Protocol-2 but the extent is a bit less as compared to Protocol-1. Following Protocol-3 we see that the height of the second peak is always larger compared to the first one signifying a structured microscopic arrangement. Though we see a flattening in the peak height between 100° and 110° for

Protocol-3 yet the extent of flattening is lesser compared to the other protocols used. This explains the active participation of chloride ions as one of the partners as its concentration increases.

References

(1)   Shaukat, S.; Buchner, R. Densities, Viscosities [from (278.15 to 318.15) K], and Electrical Conductivities (at 298.15 K) of Aqueous Solutions of Choline Chloride and Chloro-Choline Chloride. *J. Chem. Eng. Data* **2011**, *56* (12), 4944–4949.

(2)   Clark, G. N. I.; Cappa, C. D.; Smith, J. D.; Saykally, R. J.; Head-Gordon, T. The Structure of Ambient Water. *Mol. Phys.* **2010**, *108* (11), 1415–1433.

(3)   Hernández De La Peña, L.; Kusalik, P. G. Quantum Effects in Liquid Water and Ice: Model Dependence. *J. Chem. Phys.* **2006**, *125* (5), 054512.

(4)   Wilson, K. R.; Rude, B. S.; Catalane, T.; Schaller, R. D.; Tobin, J. G.; Co, D. T.; Saykally, R. J. X-Ray Spectroscopy of Liquid Water Microjets. *J. Phys. Chem. B* **2001**, *105* (17), 3346–3349.

(5)   Sarkar, S.; Maity, A.; Chakrabarti, R. Microscopic Structural Features of Water in Aqueous-Reline Mixtures of Varying Compositions. *Phys. Chem. Chem. Phys.* **2021**, *23* (6), 3779–3793.

(6)   Maity, A.; Sarkar, S.; Theeyancheri, L.; Chakrabarti, R. Choline Chloride as a Nano-Crowder Protects HP-36 from Urea-Induced Denaturation: Insights from Solvent Dynamics and Protein-Solvent Interactions. *ChemPhysChem* **2020**, *21* (6), 552–567.

(7)   Galamba, N. Water's Structure around Hydrophobic Solutes and the Iceberg Model. *J. Phys. Chem. B* **2013**, *117* (7), 2153–2159.

(8)   Giovambattista, N.; Debenedetti, P. G.; Sciortino, F.; Stanley, H. E. Structural Order in Glassy Water. *Phys. Rev. E* **2005**, *71* (6), 061505.

(9)   Chatterjee, S.; Debenedetti, P. G.; Stillinger, F. H.; Lynden-Bell, R. M. A Computational Investigation of Thermodynamics, Structure, Dynamics and Solvation Behavior in Modified Water Models. *J. Chem. Phys.* **2008**, *128* (12), 124511.

(10)   Chau, P.; Hardwick, A. J. A New Order Parameter for Tetrahedral Configurations. *Mol. Phys.* **1998**, *93* (3), 511–518.

(11)   Errington, J. R.; Debenedetti, P. G. Relationship between Structural Order and the Anomalies of Liquid Water. *Nature* **2001**, *409* (6818), 318–321.